SOILS AND FOUNDATIONS Vol. 39, No. 4, 35-45, Aug. 1999
Japanese Geotechnical Society

# SOIL-PILE INTERFACE MODEL FOR AXIALLY LOADED SINGLE PILES

EDUARDO ROJAS[i], CELESTINO VALLE[ii] and MIGUEL P. ROMO[iii]

## ABSTRACT

On the basis of the observed experimental behavior of axially loaded friction piles driven in soft clays, a soil-pile interface model is proposed using the basic rheological units: springs, dashpots and sliding elements. All the mass of soil affected by the presence of the pile is concentrated in a ring of infinitesimal width. Therefore, all the phenomena regarding the soil-pile stress distribution and displacements will take place in this surface.

The proposed rheological model is introduced in a general boundary elements formulation for axially loaded piles. In this formulation, the pile is discretized in a certain number of elements in order to consider a variety of phenomena such as: the deformation of the pile, the increment of radial and axial stresses in the soil mass due to load transfer and the stiffness of the different layers it passes across.

Parameters of the rheological model can be obtained from a creep triaxial test and a direct shear test. In case the pile cuts through different layers, it is necessary to compute the parameters for each layer.

The proposed model is able to simulate the load-displacement behavior of axially loaded floating piles subject to monotonic as well as cyclic loading. It is also possible to determine the load and displacement at the pile tip and shear stress distribution along the pile shaft.

Results of the proposed model have been compared with a very well documented series of pile tests carried out in Mexico City. Tested piles were squared 30 cm on the side and were driven 10 m in a quite homogeneous clay layer. From these comparisons it can be concluded that the model is able to adequately reproduce the most important aspects of the load-displacement behavior of friction piles driven in clay deposits.

**Key words:** axial load, friction pile, rheological units, soil-pile interface model (**IGC**: C7/H1/T12)

## INTRODUCTION

Different methods of analysis have been proposed to estimate the load-displacement behavior of friction piles. Due to space limitations, the characteristics of some of the pioneering methods are briefly discussed herein. All these methods consider the general principles of equilibrium and displacements compatibility between pile and soil.

*t-z curves.* This method uses typical shear stress-displacement curves at different depths obtained experimentally (Coyle and Reese, 1966) or analytically (Kraft et al., 1981 (a)). Considering certain hypotheses as to the strength of the soil, the analysis can be applied to normally consolidated as well as overconsolidated soils.

*Boundary elements.* Based on Mindlin's equation, two main approaches can be used: one where pile and soil boundaries are discretized (Butterfield and Banerjee, 1971) and a simplified analysis where only the pile is discretized (Mattes and Poulos, 1969). This procedure can be easily extended to pile groups.

*Rheological models.* Rheological units are used to model the pile-soil interface. In one of the first attempts, Iwan's model was used to simulate the load-displacement behavior of friction piles subject to static and cyclic axial loading (Goulois, 1982). However, this model requires an important number of parameters for each layer and it does not consider the interaction among the different sections of the pile. Results of the model were not compared with field test.

*Approached closed form solutions.* By means of some simplifying assumptions concerning the load transfer into the soil mass (considered as elastic), an approached solution is established (Randolph and Wroth, 1978). This procedure may consider radial and vertical heterogeneities.

*Finite element method.* In this approach the soil shear stress-displacement behavior is introduced by means of the hyperbolic model and the relative displacements between pile and soil are allowed by special soil-pile interface elements (Ellison et al., 1971; Desai, 1974). In the case of driven piles, initial stresses in the field can be con-

i) Professor, Universidad Autónoma de Querëtaro, Ciudad Universitaria, Querëtaro, Mëxico (formerly at Instituto de Ingeniería, UNAM).
ii) Research Engineer, Instituto Mexicano del Petróleo, Eje Central Lázaro Cárdenas #152, Mëxico, D.F. (formerly at Instituto de Ingeniería, UNAM).
iii) Professor, Instituto de Ingeniería, Universidad Nacional Autónoma de Mëxico (UNAM), Ciudad Universitaria, Mëxico, D.F.
Manuscript was received for review on December 8, 1997.
Written discussions on this paper should be submitted before March 1, 2000 to the Japanese Geotechnical Society, Sugayama Bldg. 4F, Kanda Awaji-cho 2-23, Chiyoda-ku, Tokyo 101-0063, Japan. Upon request the closing date may be extended one month.

sidered.

Each one of the models described above can simulate some of the fundamental aspects of the behavior of friction piles. These aspects are discussed below.

*Behavior of Axially Loaded Single Friction Piles*

According to tests results, the behavior of axially loaded friction piles driven in clayey soils can be described as follows:

a) A linear load-displacement behavior up to 70% of the failure load (Fig. 1, Rivera, 1982).
b) Stiffness and failure load of a floating pile highly depend on the loading rate (Fig. 2, Kraft et al., 1981 (a)). Linearity of the curves for fast loading tests persists up to 80% of the failure.
c) The stiffness of a floating pile during cyclic loading is similar to that observed for a fast loading test. On the other hand, plastic displacements accumulate with every cycle when the static failure load is exceeded.

To account for the plastic displacements that accumulate during earthquake-type loads, a model which includes the soil-pile interface behavior is proposed in this paper. The interface is modeled by means of rheological units that permit computation of elastic and plastic displacements, as well as the rate loading effects. The implementation of the procedure follows closely the method based on boundary elements proposed by Mates and Poulos (1969) and Poulos (1979).

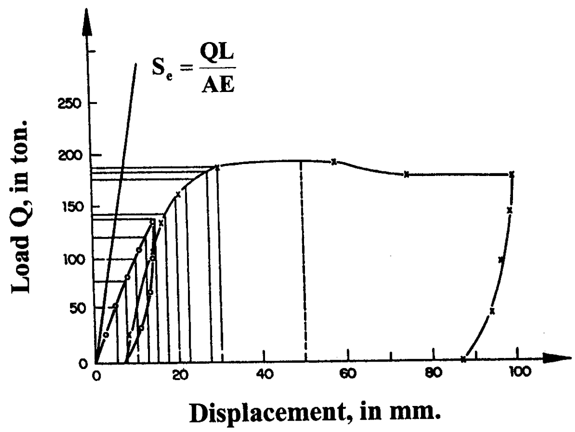


**Fig. 1. Loading tests in piles (Rivera, 1982)**

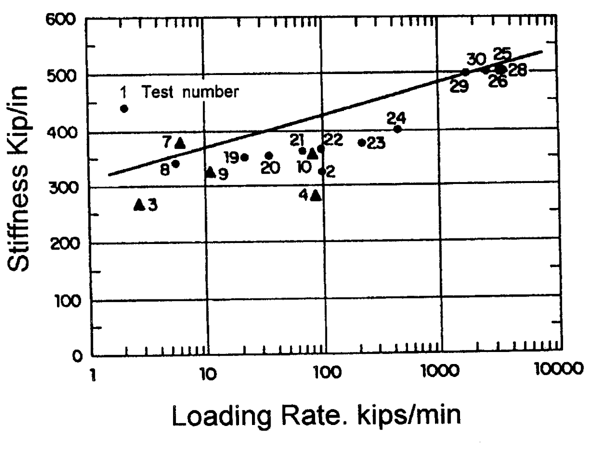


**Fig. 2. Loading rate effect (Kraft et al., 1981 (b))**

## SHEAR STRESS SOIL BEHAVIOR

A vertical floating pile subject to axial loading transmits most of its load by the friction generated between the shaft and the soil. Soil behavior under these conditions is usually simulated in the laboratory by direct shear tests. The main differences between this test and field conditions are: a) horizontal stresses (which represent the vertical stresses in the field) can not be controlled during the test; b) the horizontal confinement of the specimen (which represents the vertical direction in the field) is rigid, avoiding any displacement in that direction, while, soil in the field suffers important vertical displacements. Accordingly, one should be cautious when using data from direct shear tests for friction pile capacity calculations.

## SOIL-PILE INTERFACE MODEL

The model for the interface soil-pile behavior proposed in this paper, includes the following assumptions:

1) The total displacement of a pile can be obtained by the addition of a viscoelastic part and a viscoplastic one

$$\delta=\delta_e+\delta_p. \quad (1)$$

Viscoelastic displacements are generated by the pile load distribution into the soil. Viscoplastic displacements are produced by relative sliding between pile and soil when the residual shear strength of the soil is surpassed.

2) All the soil affected by the pile load transfer is concentrated in an infinitesimal wide ring surrounding the pile. This ring also corresponds to the sliding surface where viscoplastic displacements take place.

3) It is considered that all the loading process occurs in undrained conditions unless the loading rate is excessively slow.

4) It is assumed that a three parameter model (Fig. 3(a)) is adequate to determine the viscoelastic component of the displacement as a function of the loading history. Parameters of this model can be established from a creep triaxial test.

5) Viscoelastic displacements can be determined using Mindlin's solution for a loading point inside a semi-infinite space where the soil modulus used is evaluated from the three parameter model, as shown later.

6) Viscoplastic displacements start developing until the residual shear strength of the soil is surpassed in every section of the pile. This assumption is supported by the results of direct shear tests carried out on Mexico City clays on soil-concrete interfaces (Ovando, 1995), some of which are depicted on Fig. 4. As can be observed, the residual strength obeys Coulomb's equation, so its value will depend on the horizontal stresses existing at the pile

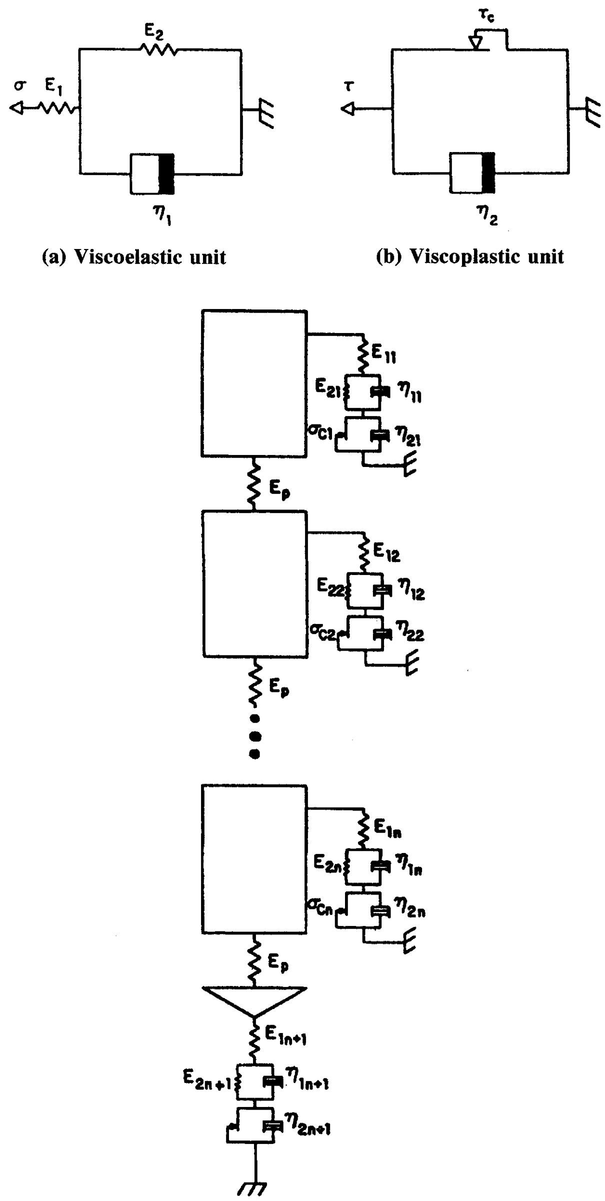


(c) Schematic representation of the complete pile-soil model

**Fig. 3. Proposed model**

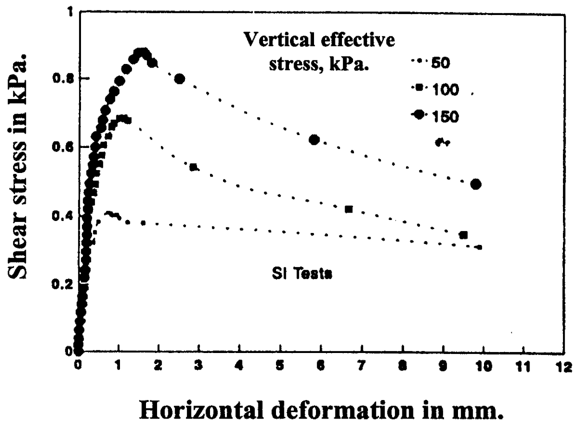


**Fig. 4. Direct shear tests results (Ovando, 1995)**

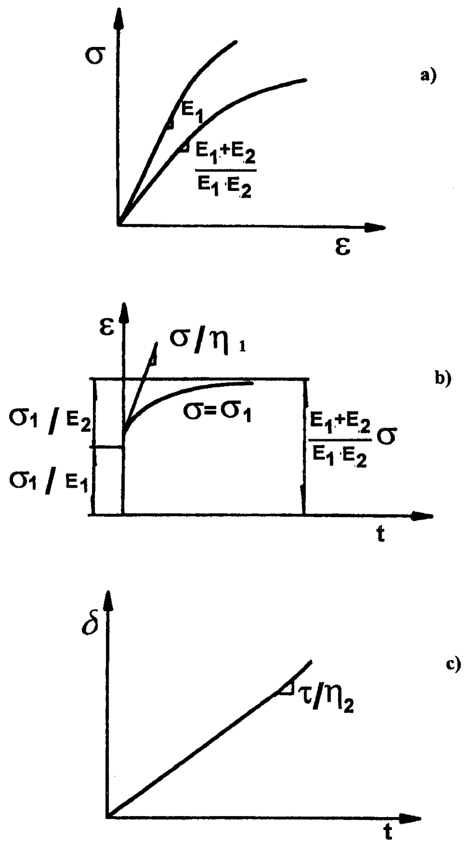


**Fig. 5. Determination of the model's parameters**

shaft at each depth. According to the viscoplastic unit (Fig. 3(b)), this assumption implies that for an infinitely slow test, failure will arise at the residual strength.

7) It is considered that a model consisting of a dashpot and a sliding mass coupled in parallel (Fig. 3(b)), is adequate to determine the viscoplastic deformation as a function of the loading rate. Parameters of this model can be established from a direct shear test.

According to the above considerations the modeling of a friction pile subject to axial loading is carried out in the following way: from the three parameter model the soil modulus at each depth is established as a function of the loading history in that zone. Thus, from Mindlin's equation the viscoelastic displacement at each depth can be obtained. If the residual shear strength is exceeded in every section of the pile, then the viscoplastic displacements are added to the viscoelastic ones to obtain the total displacement of the pile. A schematic representation of the complete model is given in Fig. 3(c).

The three parameter model proposed for the viscoelastic deformation exhibits the following particularities: under instantaneous loading only the spring $E_1$ deforms. If load persists during a certain time then the dashpot $\eta_1$ starts to deform interacting with the spring $E_2$ producing important strain rate variations. When loading persists for a very long time ($t \to \infty$) the behavior of the model is similar to springs $E_1$ and $E_2$ coupled in serial (Fig. 5(a)). Parameters $E_1$, $E_2$ and $\eta_1$ can be easily found from a creep triaxial test as shown in Fig. 5(b). On the other hand, parameter $\eta_2$ is related to the plastic displacement rate obtained from a stress controlled direct shear test when the residual strength of the soil has been surpassed (Fig. 5(c)). Plastic displacements are obtained by subtracting the elastic displacements from the total ones. In this case, the elastic modulus can be obtained from the first load increment applied on the direct shear test as long as it represents a small part (one fifth to one tenth) of the shear strength of the soil sample.

According to results of some direct shear tests carried out on Mexico City clay (Ovando, 1995), an adequate relationship for the shear strength in a soil to soil interface is given by

$$\sigma_{ci}=c_i+\sigma'_{vi}\tan\varphi_i \tag{2}$$

where $\sigma'_{vi}$ represents the effective normal stress applied on the failure surface, and $\varphi_i$ and $c_i$ are the internal friction angle and the cohesion of the soil, respectively. The same kind of relationship holds for the residual strength of the soil.

In the following sections, the relationships defining the behavior of the viscoelastic and viscoplastic models are established.

*Monotonic Loading*

First of all, equations for the viscoelastic model will be developed, following those for the viscoplastic part.

The general equation for the three parameter model shown in Fig. 3(a) is

$$\left(\frac{\eta_1}{E_1}\right)\dot{\sigma}+\left(\frac{E_1+E_2}{E_1}\right)\sigma=\eta_1\dot{\varepsilon}+E_2\varepsilon. \tag{3}$$

From this relation the viscoelastic strain ($\varepsilon_e$) at time $t$ produced by stress $\sigma(t)$ is given by

$$\varepsilon_e(t)=\frac{\sigma(t)}{E_1}+\frac{1}{\eta_1}\int_0^t \sigma(t')A\,dt' \tag{4}$$

where

$$A=\exp\left(\frac{E_2}{\eta_1}(t'-t)\right)$$

and $t'$ represents the time variable between the limits *0* and $t$. According to this expression, the displacement at time $t$ will depend on the stress history applied up to that time. If a monotonic loading is applied at constant rate of magnitude $a$, then the strain at time $t$ is given by

$$\varepsilon_e(t)=\frac{at}{E_1}+\frac{a}{E_2}\left[t-\frac{\eta_1}{E_2}(1-B)\right]$$
$$B=\exp\left(-\frac{E_2}{\eta_1}t\right). \tag{5}$$

For a creep test ($\sigma=constant$), the solution to Eq. (3) is

$$\varepsilon_e(t)=\sigma\left[\frac{E_1+E_2}{E_1E_2}\right]-\frac{\sigma}{E_2}B. \tag{6}$$

During a pile test, the total load is usually applied at small increments and constant time intervals. In consequence, loading history in this case can be considered as the superposition of a series of creep tests and therefore Boltzman's superposition principle can be applied in the form

$$\varepsilon(t)=\sigma_0J(t)+\int_0^t J(t-t')\frac{d\sigma}{dt}dt \tag{7}$$

where $\varepsilon(t)$ represents the strain at instant $t$, $\sigma_0$ the initial stress, $J(t)$ the creep function at time $t$ and $t'$ the instant at which a stress increment is applied. For the case of stress increments of different magnitude ($\Delta\sigma_j$) applied at a constant time interval $\Delta t$, the strain at the end of the $n^{th}$ increment is

$$\varepsilon_e(t)=\frac{E_1+E_2}{E_1E_2}\sum_{i=1}^{n}\Delta\sigma_i-\frac{1}{E_2}\left(\sum_{i=1}^{n}\Delta\sigma_iC\right) \tag{8}$$

where

$$C=\exp\left(-\frac{E_2}{\eta_1}(n-i+1)\Delta t\right).$$

This equation can be used to simulate a pile test at a constant loading rate. It should be stressed that even if the load increment remains constant, the stress distribution along each section of the pile shaft will be different. Furthermore, even if the values of $\Delta\sigma_i$ and $\Delta t$ remain constant, the strain response of the model is non linear.

As the model stiffness depends on the loading history, the viscoelastic tangent modulus ($E_e=(\partial\sigma_n/\partial\varepsilon_n)$) should be determined by

$$E_e=\frac{1}{\dfrac{E_1+E_2}{E_1E_2}+\dfrac{1}{E_2}\left[(1-D)\left(\sum_{i=1}^{n-1}\dfrac{\Delta\sigma_i}{\Delta\sigma_n}W\right)-D\right]} \tag{9}$$

where

$$D=\exp\left(-\frac{E_2}{\eta_1}\Delta t\right)$$
$$W=\exp\left(-\frac{E_2}{\eta_1}(n-i)\Delta t\right).$$

When shear stresses reach the residual strength ($\sigma\geq\sigma_r$), the viscoplastic unit of the model will start moving and relative displacements between pile and soil will develop. The general equation for the viscoplastic unit (Fig. 3(b)) is

$$\dot{\delta}_p=(\sigma-\sigma_r)/\eta_2,\quad \text{when}\quad \sigma-\sigma_r>0 \tag{10}$$

where $\dot{\delta}_p$ represents the viscoplastic displacement rate. Then, the displacement occurring at time $t$ is

$$\delta_p(t)=\frac{1}{\eta_2}\int_{t_0}^{t}(\sigma(t)-\sigma_r)dt \tag{11}$$

where $t_0$ represents the instant at which the applied stress $\sigma(t)$ reaches the residual strength $\sigma_r$. If the applied stresses increase at constant rate of magnitude $a$, the displacements will be given by

$$\delta_p(t)=\frac{a}{2\eta_2}(t-t_0)^2. \tag{12}$$

For creep test conditions, Eq. (11) yields

$$\delta_p(t)=\frac{1}{\eta_2}(\sigma-\sigma_r)(t-t_0). \tag{13}$$

Finally, for stress increments of different magnitude ($\Delta\sigma_j$) applied at constant time interval $\Delta t$, the displacements are computed with

$$\delta_p(t)=\frac{\Delta t}{\eta_2}\sum_{j=1}^{n}\Delta\sigma_l(n-j+1) \tag{14}$$

where $n$ represents the number of stress increments applied up to time $t$ and $l$ the stress increment number for which $l\Delta\sigma=\sigma_r$.

*Behavior under Cyclic Loading*

Herein the behavior of the proposed model for the case of cyclic loading is presented. It is considered that the soil does not degrade due to cyclic loading. This approximation may not be adequate for many low to medium plasticity clays, however there exists an increasing bulk of experimental evidence (i.e. Romo, 1995) that shows that the highly plastic Mexico City clays undergo negligible degradation when loaded by as many as 50 cycles with dynamic stresses as high as 80% of the clay undrained strength. Thus, this model limitation is of little practical concern for highly plastic clays similar to those of Mexico City. For other less plastic clays, degradation effects should be accounted for. The model may readily be modified to reproduce such effects.

Consider a cyclic stress of the form

$$\sigma=\sigma_{cy}\sin(\omega t) \tag{15}$$

acting on the model presented in Fig. 3(a), where $2\sigma_{cy}$ represents the amplitude of the cyclic loading, $\omega$ the frequency and $t$ the time; viscoelastic strains are given by (Flügge, 1968)

$$\varepsilon_e(t)=\sigma_{cy}(E_{c1}\sin(\omega t)+E_{c2}\cos(\omega t)) \tag{16}$$

where

$$E_{c1}=\frac{\dfrac{E_1E_2}{E_1+E_2}+\left(\dfrac{\eta_1E_2}{E_1+E_2}\right)^2\dfrac{\omega^2}{E_1}}{\left(\dfrac{E_1E_2}{E_1+E_2}\right)^2+\left(\dfrac{\eta_1E_2}{E_1+E_2}\right)^2\omega^2} \tag{17}$$

$$E_{c2}=\frac{\left[\dfrac{E_2}{E_1+E_2}-\left(\dfrac{E_2}{E_1+E_2}\right)^2\right]\eta_1\omega}{\left(\dfrac{E_1E_2}{E_1+E_2}\right)^2+\left(\eta_1\dfrac{E_2}{E_1+E_2}\right)^2\omega^2} \tag{18}$$

and the tangent modulus is

$$E_e=\cos(\omega t)/(E_{c1}\cos(\omega t)-E_{c2}\sin(\omega t)). \tag{19}$$

If $\sigma\geq\sigma_r$, viscoplastic displacements will take place. These displacements can be determined from the analysis of the viscoplastic unit (Fig. 3(b)) considering that it undergoes a cyclic loading which reaches the critical value $\sigma_r$ at instant $t_0$. Under these conditions

$$\delta_p(t)=(\sigma_{cy})\left(\frac{\cos(\omega t_0)-\cos(\omega t)}{\eta_2\omega}\right)+\frac{\sigma_{st}-\sigma_r}{\eta_2}(t-t_0) \tag{20}$$

where the cosine argument is given by

$$\omega t_0=\sin^{-1}[(\sigma_r-\sigma)/\sigma_{cy}]. \tag{21}$$

Here $\sigma$ represents the sum of the static and the cyclic stresses given by

$$\sigma=\sigma_{st}+\sigma_{cy}\sin\omega t. \tag{22}$$

## SOIL-PILE SYSTEM

The model presented here is based on the simplified boundary elements method proposed by Poulos (1979) for axially loaded piles. However, in the present model the pile-soil interface behavior is represented by means of the viscoelastic modulus that takes into account the rate and duration of loading.

To set up the problem, the pile is divided into a number of small sections and the viscoelastic behavior of the soil surrounding the pile is represented by the three parameter model. The relationship between stresses on the pile shaft and viscoelastic soil displacements is established by means of Mindlin's equation. In the case of stratified soil, parameters of the model should be determined for each layer. The applied load is distributed along the pile shaft by assuming a tip displacement and by considering the compatibility between pile and soil displacements. If equilibrium is not reached with this distribution, the load is redistributed along the pile shaft by assuming another tip displacement. This process is repeated until equilibrium and compatibility are fulfilled. In order to take account of the loading rate the model is formulated in the time domain. Accordingly, the model would be able to simulate the load-displacement behavior of a floating pile for monotonic loads applied at different loading rates or cyclic loads applied at different frequencies.

Displacements of the pile are computed at the pile shaft or at a small distance from it when a crust of soil appears. This surface represents the interface of infinitesimal width mentioned above, where all the phenomena associated with the soil take place. As suggested by Poulos (1968, 1979, 1980), these displacements may be computed with:

$$\{ds\}=[I_D]\{d\sigma\} \tag{23}$$

where $\{ds\}$ represents the soil displacement vector at each node and $[I_D]$ is Mindlin's influence factors matrix. This matrix is formed by the mid-height displacements produced by the loads acting on each one of the sections of the pile and divided by the shear stress at each section. These displacements can be obtained considering that the axial load on a pile section is distributed into the soil as a uniform shear stress around the section's perimeter. In that case the influence factor can be obtained by integration of Mindlin's equation along a section of the pile as performed by Poulos (1968).

Once the influence factors are defined, the viscoelastic displacements, $\delta_e$, are computed following the iteration procedure developed by Poulos (1968, 1979, 1980).

To compute the corresponding viscoplastic displacements, it is necessary first to evaluate the residual or critical shear strength at each node of the pile. This strength can be obtained from Eq. (2) written in the form

$$\sigma_{ri} = c_{ri} + (K_i \sigma_z + d\sigma_r - u_z) \tan \varphi_{ri} \tag{24}$$

where $c_{ri}$, $\varphi_{ri}$ and $K_i$ represent the residual cohesion, the residual internal friction angle and the lateral earth pressure coefficient of the soil at level $i$, respectively; $\sigma_z$, $d\sigma_r$ and $u_z$ represent the total vertical stress, the radial stress increment given by Mindlin's solution and the pore water pressure at depth $z$, respectively.

According to Eq. (24), pile bearing capacity increases with the applied load as radial stresses grow with each load increment. Once the critical stress is surpassed, displacements tend to increase rapidly.

The critical bearing capacity of the pile base (where $z = l_p$, pile length) is considered to be given by

$$\sigma_{pr} = 9c_{ri} + \sigma_z + d\sigma_z - u_z \tag{25}$$

where $d\sigma_z$ is the vertical stress increment at base depth. This increment is also computed using Mindlin's solution.

## LABORATORY SOIL TEST REQUIRED

Soil parameters $E_1$, $E_2$, $\eta_1$ and $\eta_2$ can be obtained from two ordinary laboratory tests. For $E_1$, $E_2$ and $\eta_1$, a creep triaxial test is needed. While determination of parameter $\eta_2$ requires a stress controlled direct shear test. The creep test should be performed using small stress increments so that the results can be used to evaluate the viscoelastic behavior of the soil. In general, a load increment of one fifth to one tenth of the failure load is adequate. Special care should be taken on the loading system of the triaxial chamber in order to avoid or minimize the influence of friction.

For the direct shear test, several load increments are needed. The sample should be loaded beyond the residual strength as it has been stated that plastic displacements appear solely when the residual shear strength of the soil is surpassed. The first load increment describes the viscoelastic behavior of the soil and therefore a small load increment (one fifth to one tenth of the failure load) is required. Viscoplastic displacements can be obtained by subtracting from the total displacements the elastic ones resulting from the first load increment. Additional direct shear tests of the strain controlled type provide the residual shear strength parameters $\varphi_{ri}$ and $c_{ri}$. In the presence of water, piezometric measurements at different depths along the pile are needed to determine the pore pressure distribution.

On the other hand, and according to the third hypothesis of the model, for most cases (unless the pile loading process is excessively slow) it can be assumed that $\nu_i = 0.5$. Finally, the value of $K_i$ should be established. The best way of doing this is by direct measurements at the site; when this is not possible one may resort to empirical correlations (Mayne and Kulhawy, 1982). It should be mentioned that in applying these correlations, due consideration to the effects of preboring and pile driving should be given.

## CONSIDERATIONS OF PILE DRIVING ON SOIL PARAMETERS

Pile driving operations induce important changes in the initial conditions of the soil influencing the behavior of friction piles. Some of the most important phenomena involved during pile driving are the following.

1) A radial stress relaxation on the walls of the hole when preboring is performed.
2) Downdrag and plastification of soil around the pile shaft during driving.
3) Pore pressure increase in saturated soils.
4) Reconsolidation of the soil due to pore pressure dissipation.
5) In the case of concrete piles, adherence of a fine crust of material.
6) Development of positive and negative residual friction loads once the pile has been installed.

The complexity of the phenomena described above makes it very difficult to take into account each one of them during the analysis. On the other hand, soil samples are usually taken from the site before piles have been driven, therefore parameters obtained from these samples may not represent the current conditions of the soil, as has been reported by several researchers. For example, Marsal et al. (1953) observed that the shear strength of the soil nearer to the shaft is reduced half its original strength just after pile driving. Thereafter, the soil started to gain strength with a tendency to its original value. Zeevaert (1973) reported that highly plastic preconsolidated soils could lose 60% of their original strength. Orrje and Broms (1967) observed that sensitive clayey soils regain their original strength some months after the driving. Finally, Peck (1965) reported that for some materials the original strength of the soil could be surpassed after a certain time. Even if these observations may seem contradictory, they simply indicate that the strength regain of a remolded soil will be highly dependent on the driving process and type of soil. Therefore, it cannot be easily estimated without an ample experimental program.

To show the influence of parameter values on model be-

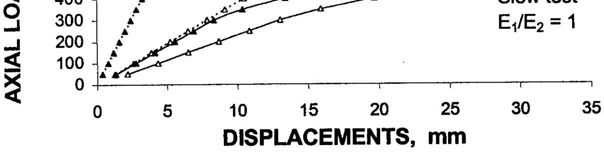


Fig. 6. Influence of ratio $E_1/E_2$

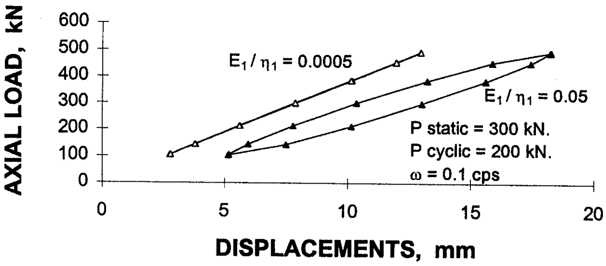


**Fig. 7. Influence of parameter $\eta_1$**

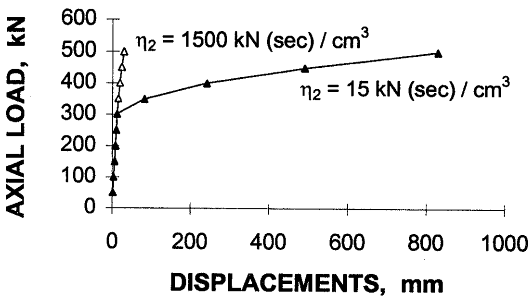


**Fig. 8. Influence of parameter $\eta_2$**

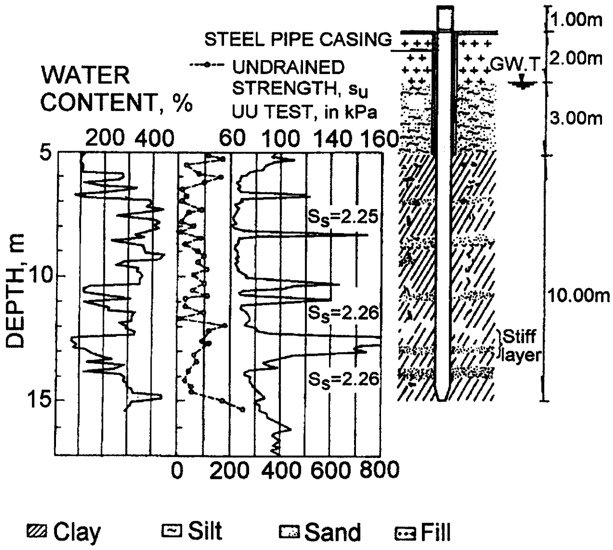


**Fig. 9. Test site (from Jaime, Romo, Reséndiz, 1990)**

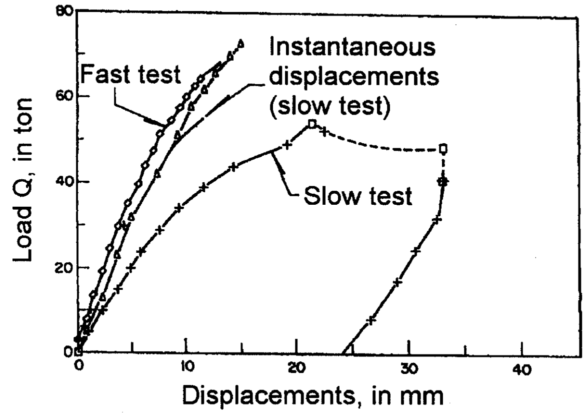


**Fig. 10. Monotonic loading tests**

havior Figs. 6 to 8 are presented. In Fig. 6 the influence of ratio $E_1/E_2$ varying from 1 to 10 for slow ($t$=2 hr/inc) and fast ($t$=4 sec/inc) rate tests can be observed. As the ratio $E_1/E_2$ increases, pile behavior becomes stiffer. On the other hand $\eta_1$ is responsible for energy dissipation as can be observed in Fig. 7. More energy is dissipated as the ratio $E_1/\eta_1$ reduces from 0.0005 to 0.05. Finally, as observed in Fig. 8, $\eta_2$ influences the plastic strain increment when the residual strength is surpassed.

## EVALUATION OF THE MODEL

In this section, theoretical results are compared with results of well documented friction pile tests carried out in Mexico City clay (Jaime et al. 1990). Square concrete piles 30 cm by side and 16 m long were used in the field tests.

### *Pile Tests*

Tests were performed in one of the areas most damaged during the 1985 earthquake in Mexico City. Figure 9 shows the site stratigraphy. From this figure it can be observed that between 5 and 15.5 m depth there are three clayey layers with water contents ranging from 250 to 450% alternated with thin sand deposits. Given that the first five meters were constituted by a very heterogeneous fill which could complicate the interpretation of the test results, it was decided to introduce a steel tube 50 cm in diameter and five meters long which would allow the pile to be in contact only with the clayey soil. In this way the effective pile length was only 10 m.

Pile loading was applied by a hydraulic jack. On top of the pile a ball and socket joint was placed in order to avoid the transmission of flexural stresses. Monotonic loading tests started four months after pile driving. Thereafter piles were left at rest for at least five weeks before cyclic loading was applied. Detailed information about the test procedure can be found in Jaime et al. (1990).

Monotonic loading tests were performed in four different piles at two loading rates: at fast rate, reaching a maximum value of 73 tons in 55 seconds and at slow rate, applying increments of 5 tons every two hours and reaching a maximum loading of 55 tons in a little more than 22 hours. During the slow rate test the "instantaneous" displacement (displacement at one minute after the load increment was applied) was registered. It is interesting to observe that when the "instantaneous" displacement is plotted against the applied load a very similar curve to the fast rate type test is obtained (Fig. 10). For the cyclic loading tests, a static load was applied prior to the 30 loading-unloading cycles. This load was applied 15 minutes before cycling.

After each cyclic loading, the pile was allowed to rest for 10 minutes, during which only the static load remained; afterwards, another 30 cycles of higher amplitude were given. This procedure was repeated until failure was reached. The frequency of the cyclic loads varied from 1 to 0.01 cycles per second due to the restraint capacity of the hydraulic pump feeding the jack.

*Test Site Parameters Determination*

Several tests were performed on undisturbed soil samples including monotonic and cyclic simple shear tests. However, no direct shear nor triaxial creep tests were carried out at that time.

Therefore, in order to obtain the missing information required by the model, a reconstituted material from soil samples of similar clay deposits was prepared. This soil was consolidated in a large consolidometer at a vertical stress corresponding to that reported at 10 m depth in the site ($\sigma_v'=55$ kPa). This practice of forming artificial soil has been used in a number of studies where it has been shown that its stress-strain-strength behavior is very similar to that of equivalent natural soil (Mendoza, 1997). The characteristics of the artificial soil (water content $w=262\%$, specific weight $\gamma_s=1.20\ \mathrm{t/m^3}$ and undrained strength $c_u=38$ kPa) were similar to those of the natural soil ($w=250\%$, $\gamma_s=1.20\ \mathrm{t/m^3}$ y $c_u=35$ kPa). Results of the creep and direct shear tests, as well as the procedures to define $E_1$, $E_2$, $\eta_1$ and $\eta_2$ are shown in Figs. 11 and 12, respectively. The values of these parameters are: $E_1=14.0$ MPa, $E_2=17.2$ MPa, $\eta_1=1.86\times10^7$ kN(sec)/cm$^3$ and $\eta_2=1270$ kN(sec)/cm$^3$. Pile elastic modulus was taken as $E_p=1.45\times10^5$ MPa; the lateral earth pressure was estimated from field test measurements carried out by Zeevaert (1957) on concrete piles in Mexico City clay $K=0.70$, the Poisson's ratio was assumed to be $\nu=0.5$, and the soil strength parameters were determined from direct shear tests on clay-concrete intefaces (Ovando, Roque, Castellanos, 1995). Their values were $\varphi_r=33^0$ and $c_r=2.0$ kPa.

*Model Versus Experimental Results*
*Monotonic tests*

Once the parameters of the model are known it is possible to simulate the behavior of axially loaded friction piles subject to different loading conditions. In Fig. 13 the theoretical and experimental results are compared for the fast and slow monotonic loading tests. These results show that the model adequately reproduces the response of the pile under slow loading conditions. However, for the case of rapid loading, the model underpredicts the initial stiffness of the soil-pile system. Nevertheless the main features of the displacement-load curve are fairly well reproduced.

It is seen that the measured capacity is accurately predicted by the model only for the slow test condition. The lower stiffnesses predicted by the model seem to be the main source of discrepancies between theoretical and experimental results. This could be explained, at least in

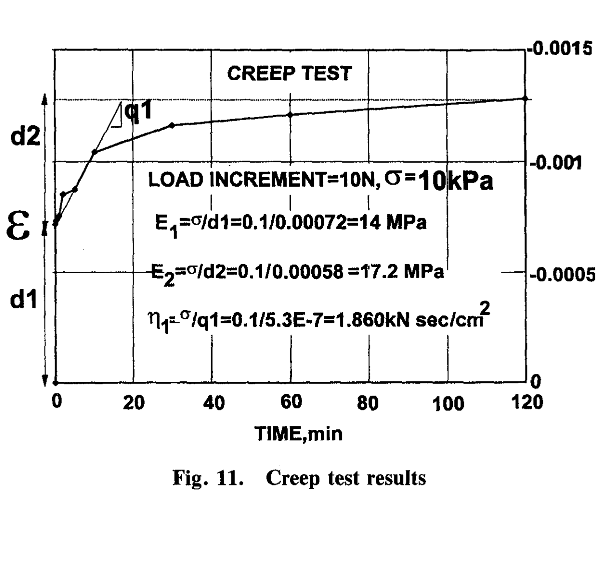


**Fig. 11. Creep test results**

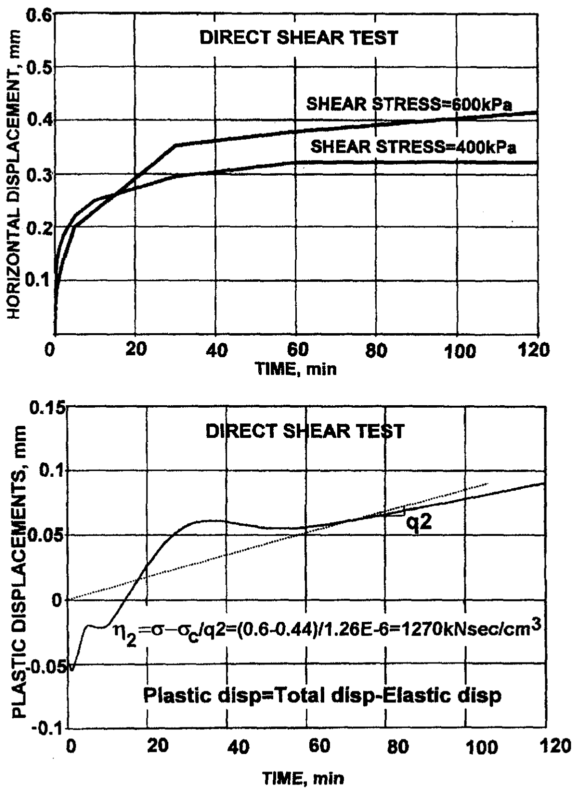


**Fig. 12. Direct shear test results**

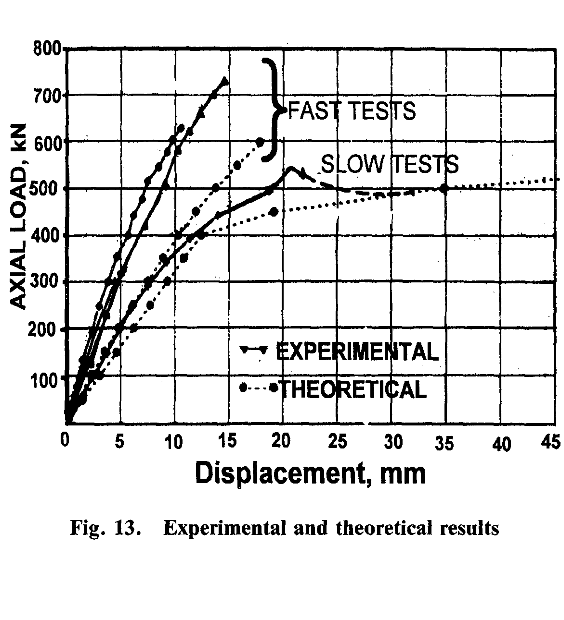


**Fig. 13. Experimental and theoretical results**

part, by the generally accepted knowledge about the stiffness increase of the soil-pile interface with time after pile driving operations. Observed behavior of an instrumented pile-box foundation in Mexico City clay lends support to this assumption (Mendoza and Romo, 1997).

*Cyclic tests*

Results of two piles tested under cyclic loading are shown in Figs. 14 to 16. Pile 1 was tested under a static load of 250 kN and a cyclic loading level of 350 kN (Fig. 14). Cyclic loading was applied during 40 cycles at the frequency indicated in each figure.

Then the pile was left to rest for a one month period. Afterwards it was monotonically loaded to a static load of 400 kN and left to reach displacement stabilization. Finally, a cyclic loading of 210 kN was applied; the results are shown in Fig. 15.

Finally Fig. 16 shows the response of pile 2 subjected to a static load of 400 kN and cyclic loading of 240 kN. The testing conditions are included in the figure.

From these comparisons it can be observed that the model reproduces adequately well the main aspects of the pile load-displacement response.

One of the most important differences for cyclic loading is that theoretical and experimental results do not start at the same displacement at the beginning of the cycling, being larger than those computed by the model.

This may be explained, at least partially, on the grounds of the lower model-predicted stiffnesses which would lead to larger plastic strains due to sustained loading. Another difference can be observed at higher cyclic loading levels where the experimental rate of plastic deformations tends to increase with every cycle, probably

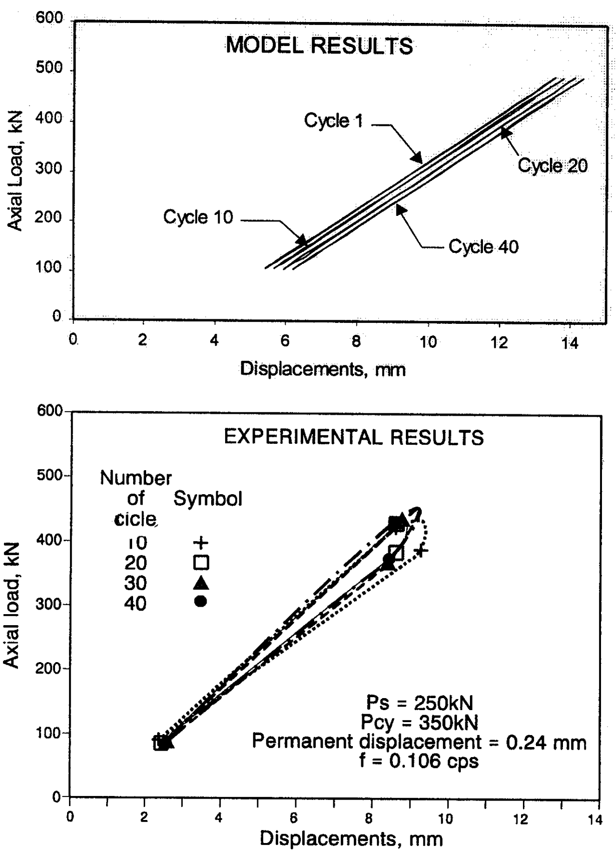


Fig. 14. Experimental and theoretical results (Pile 1)

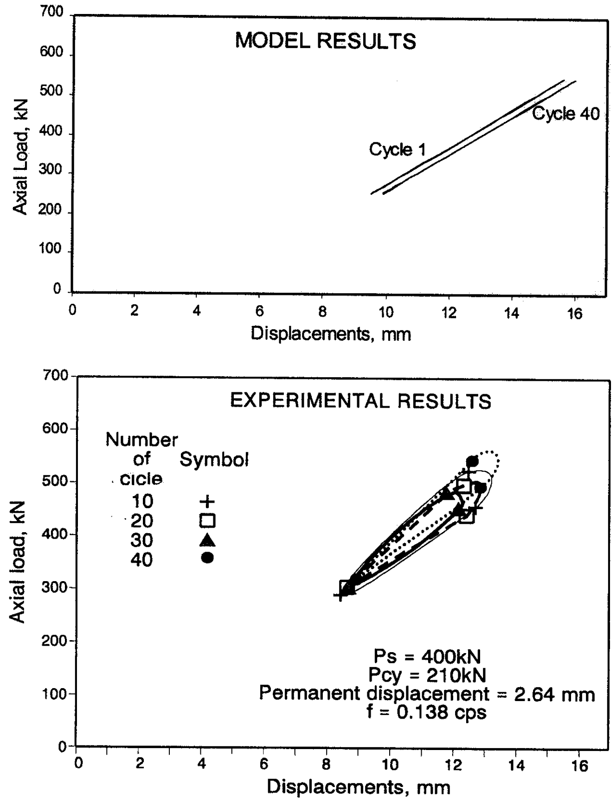


Fig. 15. Experimental and theoretical results (Pile 1)

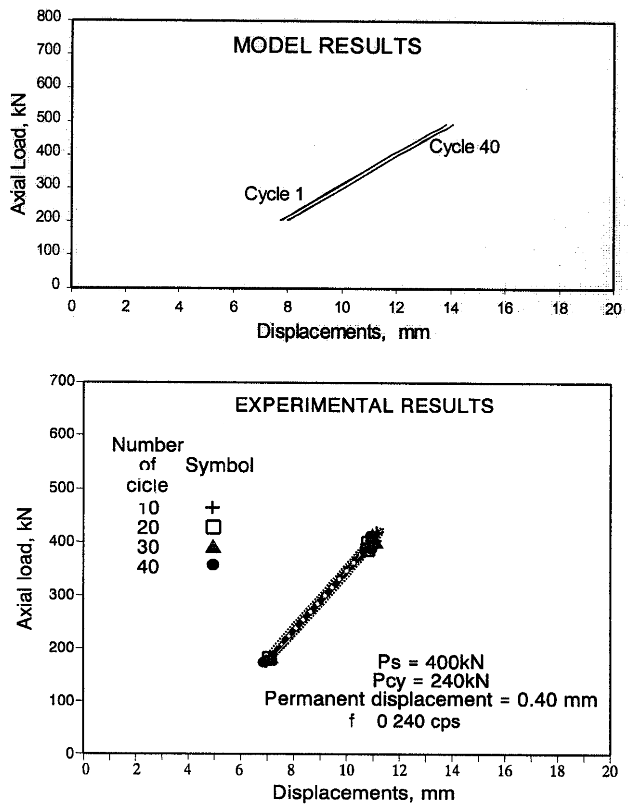


Fig. 16. Experimental and theoretical results (Pile 2)

due to some degradation of the soil properties, a phenomenon not included in the model.

## CONCLUSIONS

1. Based on the observed behavior of axially loaded friction piles, a rheological model for the pile-soil interface has been advanced. The analysis is carried out with a general formulation for friction piles based on a simplified boundary element approach, similar to that proposed by Poulos (1979).

2. Parameters of the model can be established from creep triaxial and direct shear tests. Ideally, soil samples for these tests should be retrieved from the ground near the pile shaft. However, this practice is not usually followed and parameters from undisturbed soil samples are generally used. This implies some approximations.

3. The model proposed is able to reproduce the most important aspects of the behavior of floating piles subjected to monotonic and cyclic axial loading. At its present stage, the model accounts only for cases where the load-displacement curve depicts a strain hardening behavior.

4. From the parametric study it was observed that an increase of the order of 30% in the values of $E_1$ and $E_2$ allowed a much better correspondence between theoretical and experimental results. This would support the idea that the soil near the pile becomes stiffer because of the consolidation phenomenon.

## NOTATION

| | |
|---|---|
| $A_L$ | Lateral area of each section of the pile |
| $A_T$ | Cross section of the pile |
| $c$ | Depth of load in Mindlin's solution |
| $c_{ri}$ | Residual soil cohesion at level $i$ |
| $CP(i,j)$ | Pile compression matrix |
| $db$ | Pile tip displacement |
| $dh_i$ | Vertical deformation of section $i$ of the pile |
| $dl_i$ | Vertical deformation increment of section $i$ of the pile |
| $dP_i$ | Vertical load increment in section $i$ of the pile |
| $ds_i$ | Soil displacement increment at level $i$ |
| $dz$ | Vertical displacement of the soil at depth $z$ |
| $e$ | Base of natural logarithm |
| $E_p$ | Pile elastic modulus |
| $E_s$ | Soil elastic modulus |
| $E_1, E_2$ | Parameters of the viscoelastic part of the model related to the elastic modulus of the soil |
| $E_t$ | Tangent elastic modulus |
| $Ip(i,j)$ | Deformation factor at level $i$ produced by a load applied at level $j$ |
| $K_i$ | Lateral earth-pressure coefficient at level $i$ |
| $l$ | Number of load increments of magnitude $\Delta\sigma$ such that $l\Delta\sigma=\sigma_r$ |
| $l_p$ | Pile length |
| $l_s$ | Length of each section of the pile |
| $n$ | Number of load increments applied up to time $t$ |
| $N$ | Number of sections of the pile |
| $N_{cy}$ | Number of loading cycles |
| $P$ | Applied load at depth $c$ in Mindlin's solution |
| $r_0$ | Pile radius |
| $R_1, R_2$ | Radial distances in Mindlin's solution |
| $S(i,j)$ | Addition matrix |
| $t$ | Time |
| $t_0$ | Instant at which $\sigma=\sigma_r$ |
| $u_z$ | Pore pressure at depth $z$ |
| $d\sigma_r$ | Radial stress increment |
| $\Delta\sigma$ | Stress increment |
| $\delta$ | Displacement |
| $\eta_1, \eta_2$ | Soil viscous parameters |
| $\nu$ | Soil Poisson's ratio |
| $\varphi_{ri}$ | Residual friction angle at level $i$ |
| $\sigma$ | Interface stress |
| $\sigma_{cy}$ | Half the amplitude of the cyclic stress loading |
| $\sigma_r$ | Residual shear strength |
| $\sigma_{st}$ | Sustained static load |
| $\sigma_z$ | Vertical total stress |
| $\omega$ | Cyclic loading frequency |

## ACKNOWLEDGMENTS

The authors gratefully acknowledge the Instituto Mexicano del Petróleo and the Instituto de Ingeniería, UNAM, for their support provided through grant FIES-94-IV.

## REFERENCES

1) Butterfield, R. and Banerjee, P. K. (1971): "The elastic analysis of compressible piles and pile groups," Géotechnique, Vol. 21, pp. 43–60.
2) Coyle, H. M. and Reese, L. C. (1966): "Load transfer for axially loaded piles in clay," J. SMF Div., ASCE, Vol. 92, SM2, pp. 1–25.
3) Desai, C. S. (1974): "Numerical design-analysis for piles in sands," J. Geotech. Engrg. Div., ASCE, Vol. 100, No. GT6, pp. 613–635.
4) Ellison, R. D., D'Appolonia, E. and Thiers, G. R. (1971): "Load deformation mechanism for bored piles," J. SMF Div., ASCE, Vol. 97, SM4, pp. 661–678.
5) Flügge, W. (1967): Viscoelasticity, Blaisdell Publishing Company.
6) Goulois, A. M. (1982): "Contribution to the study of tension piles under cyclic loading," Ph.D. Thesis, MIT, USA.
7) Jaime, A., Romo, M. P. and Resêndiz, D. (1990): "Behavior of friction piles in Mexico City clay," J. Geotech. Engrg. Div., ASCE, Vol. 116, G-T-6, pp. 915–931.
8) Kraft, L. M., Ray, R. P. and Kawaga, T. (1981 (a)): "Theoretical $t$-$z$ curves," J. Geotech. Engrg. Div. ASCE, Vol. 107, No. G-T11, pp. 1543–1561.
9) Kraft, L. M., Cox, W. R. and Verner, E. A. (1981 (b)): "Pile load tests: cyclic loads and varying loading rates," J. Geotech. Engrg. Div., ASCE, Vol. 107, GT1, pp. 1–19.
10) Marsal, R., Mazari, M. and Hiriart, H. (1953): "Cimentaciones piloteadas en la ciudad de Mêxico" Ingeniería Experimental, ICA, serie B, Vol. 16, Mêxico.
11) Mayne, P. W. and Kulhawy, F. H. (1982): "$K_0$-OCR relationships in soil," J. Geotech. Engrg. Div., ASCE, Vol. 106, No. GT10.
12) Mattes, N. S. and Poulos, H. G. (1969): "Settlement of single compressible pile," J. SMF. Div., ASCE, Vol. 95, SM1, pp. 189–207.
13) Mendoza, M. (1997): "Thesis in partial fulfillment of the requirements to obtain the Doctor in Engineering degree," DEPFI, UNAM, Mêxico (in progress).
14) Mendoza, M. and Romo, M. P. (1997): "Performance of a friction pile-box foundation in Mexico City clay," (to be published, Soils and Foundations.)
15) Orrje, O. and Broms, B. B. (1967): "Effects of pile driving on soil properties," J. SMF. Div., ASCE, Vol. 93, SM5, pp. 59–73.
16) Ovando, E. (1995): "Direct shear tests on Mexico City clay with reference to friction pile behaviour," J. Geotech. and Geological Engrg., Vol. 13, pp. 1–16.
17) Ovando, E., Roque, G. and Castellanos, J. E. (1995): "Direct shear tests in Mexico City clay," A Partial Report to the European Economic Community, Contract No CI1-CT93-0046 (DG 12

HSMU), Seismic Behavior of Piles, March 1995.
18) Peck, R. B. (1958): "A study of the comparative behaviour of friction piles," Special Report 36, Highway Research Board, Washington, DC, 10-11.
19) Poulos, H. G. and Davis, E. H. (1968): "The settlement behaviour of single axially loaded incompressible piles and piers," Gêotechnique, Vol. 18, pp. 351-371.
20) Poulos, H. G. (1979): "Development of an analysis for cyclic axial loading of piles," 3rd Int. Conf. Num. Methods in Geomechanics, Aachen, pp. 1513-1530.
21) Poulos, H. G. and Davis, E. H. (1980): Pile Foundation Analysis and Design, (ed.), John Wiley & Sons, New York, USA.
22) Randolph, M. F. and Wroth, C. P. (1978): "Analysis of deformation of vertically loaded piles," J. Geotech. Engrg. Div., ASCE, Vol. 104, GT12, pp. 1465-1488.
23) Rivera, R. (1982): "Discussion and interpretation of pile loading tests," Master thesis, DEPFI, UNAM, Mêxico (in Spanish).
24) Romo, M. P. (1995): "Clay behavior, ground response and soil-structure interaction studies in Mexico City," State of the Art paper, 3rd Int. Conf. on Recent Advances in Geotechnical Earthquake Engineering and Soil Dynamics, St. Louis Missouri, Vol. 2, pp. 1039-1051, April.
25) Seed, B. and Reese, L. C. (1955): "The action of soft clay along friction piles," ASCE Transactions, Paper 2882, pp. 731-764.
26) Zeevaert, L. (1973): Foundation Engineering for Difficult Subsoil Conditions, Van Nostrand Reinhold, New York, USA.